EBioMedicine 47 (2019) 436–445

Contents lists available at ScienceDirect

EBioMedicine

journal homepage: www.ebiomedicine.com

EBioMedicine
Published by THE LANCET

Salsalate, but not metformin or canagliflozin, slows kidney cyst growth in an adult-onset mouse model of polycystic kidney disease

Wouter N. Leonhard [a,1], Xuewen Song [b,e,1], Anish A. Kanhai [a], Ioan-Andrei Iliuta [b,e], Andrea Bozovic [c,f], Gregory R. Steinberg [d], Dorien J.M. Peters [a,**,2], York Pei [b,e,*,2]

[a] Department of Human Genetics, Leiden University Medical Centre, Leiden, the Netherlands
[b] Division of Nephrology, University Health Network, Toronto, Ontario, Canada
[c] Laboratory Medicine and Pathobiology, University Health Network, Toronto, Ontario, Canada
[d] Centre for Metabolism, Obesity and Diabetes Research, McMaster University, Hamilton, Ontario, Canada
[e] Division of Nephrology, University of Toronto, Toronto, Ontario, Canada
[f] Laboratory Medicine and Pathobiology, University of Toronto, Toronto, Ontario, Canada

ARTICLE INFO

Article history:
Received 31 May 2019
Received in revised form 9 August 2019
Accepted 19 August 2019
Available online 28 August 2019

Keywords:
Salsalate
Metformin
Canagliflozin
AMPK
Polycystic kidney disease

ABSTRACT

Background: Multiple preclinical studies have highlighted AMP-activated protein kinase (AMPK) as a potential therapeutic target for autosomal dominant polycystic kidney disease (ADPKD). Both metformin and canagliflozin indirectly activate AMPK by inhibiting mitochondrial function, while salsalate is a direct AMPK activator. Metformin, canagliflozin and salsalate (a prodrug dimer of salicylate) are approved for clinical use with excellent safety profile. Although metformin treatment had been shown to attenuate experimental cystic kidney disease, there are concerns that therapeutic AMPK activation in human kidney might require a higher oral metformin dose than can be achieved clinically.

Methods: In this study, we tested metformin-based combination therapies for their additive (metformin plus canagliflozin) and synergistic (metformin plus salsalate) effects and each drug individually in an adult-onset conditional *Pkd1* knock-out mouse model ($n = 20$ male/group) using dosages expected to yield clinically relevant drug levels.

Findings: Compared to untreated mutant mice, treatment with salsalate or metformin plus salsalate improved kidney survival (i.e. blood urea nitrogen <20 mmol/L at the time of sacrifice) and reduced cystic kidney disease severity. However, the effects of metformin plus salsalate did not differ from salsalate alone; and neither metformin nor canagliflozin was effective. Protein expression and phosphorylation analyses indicated that salsalate treatment was associated with reduction in mTOR (mammalian target of rapamycin) activity and cellular proliferation in *Pkd1* mutant mouse kidneys. Global gene expression analyses suggested that these effects were linked to restoration of mitochondrial function and suppression of inflammation and fibrosis.

Interpretation: Salsalate is a highly promising candidate for drug repurposing and clinical testing in ADPKD.

1. Introduction

Autosomal dominant polycystic kidney disease (ADPKD) is the most common inherited kidney disease worldwide with a life-time risk of at least 1/1000 in the general population [1]. Mutations of two genes, *PKD1* and *PKD2*, account for 75–85% and 15–25% of the genetically resolved cases [2–5]. Disease progression of ADPKD is highly variable in part due to gene locus and allelic effects with the most severe disease associated with *PKD1* protein-truncating mutations, intermediate disease severity with *PKD1* non-truncating mutations, and mild disease with *PKD2* mutations [3–5]. Progressive increase in cyst number and size with age results in distortion of the normal kidney architecture and ultimately, end stage renal disease (ESRD) in a majority of patients [6]. Additionally, non-kidney related complications such as intracranial arterial aneurysms, polycystic liver, and heart valve defect also contribute to the morbidity and mortality of this disease [7]. Overall, ADKPD accounts for 5–10% of ESRD in the developed countries.

The pathobiology of ADPKD is not well understood but a "threshold model" of cystogenesis is supported by recent studies [7–9]. Under this

* Corresponding author at: Division of Nephrology, University Health Network, Toronto, Ontario, Canada.
** Corresponding author.
E-mail addresses: D.J.M.Peters@lumc.nl (D.J.M. Peters), york.pei@uhn.ca (Y. Pei).
[1] W.N.L. and X.S. are co-first authors.
[2] D.J.M.P. and Y.P. are co-senior authors.

https://doi.org/10.1016/j.ebiom.2019.08.041

Research in context

Evidence before this study

Autosomal dominant polycystic kidney disease (ADPKD) is the most common inherited kidney disease worldwide. Previous preclinical studies showed that metformin slowed PKD progression by activating AMPK; however, translating these findings to patients might require a higher oral metformin dose than can be achieved clinically.

Added value of this study

To optimize AMPK-based therapeutic in ADPKD, we tested oral metformin-based combination therapies for their additive (metformin plus canagliflozin) and synergistic (metformin plus salsalate) effects and each drug individually in a conditional *Pkd1* knockout mouse model. Using dosages expected to yield clinically relevant serum drug levels, we found only salsalate (a pro-drug dimer of salicylate) slowed PKD progression by improving mitochondrial function and reducing inflammation.

Implications of all the available evidence

Salsalate is a promising repurposed drug for treatment of ADPKD.

model, variable reduction of cellular levels of functional polycystin-1 (i.e. the protein encoded by *PKD1*) due to germline and somatic mutations and stochastic factors, can influence cystic disease severity by modulating a complex array of signalling pathways [8–10]. However, restoration of functional polycystin-1 levels toward normal in cystic tissues presently remains an elusive therapeutic goal. By contrast, targeting key signalling pathways that drive cyst growth holds much promise for therapeutic development and clinical translation [7]. Indeed, the realization that increased cAMP signalling is a key driving mechanism for cyst growth and fluid secretion has led to the development of vasopressin V2 receptor (V2R) based therapy. Tolvaptan, an oral V2R antagonist which lowers $[cAMP]_i$ to slow cyst growth and delay loss of kidney function, has been recently approved as the first disease-modifier drug for treatment of ADPKD in multiple countries [11–15]. However, tolvaptan is an expensive drug associated with significant side-effects, rendering its use restricted to high-risk patients. There is an urgent need for developing additional treatment for ADPKD.

Multiple experimental studies have highlighted the importance of mTORC1 (mammalian target of rapamycin complex 1) activation in modulating cyst growth in ADPKD [16–22]. Notably, therapeutic mTORC1 inhibition was highly effective in preclinical studies [16–18]. However, the results of two randomized controlled clinical trials of mTORC1 inhibitors in ADPKD demonstrated that low-dose treatment was ineffective [23] while high-dose treatment was associated with severe toxicities [24]. An upstream inhibitor of the mTORC1 pathway is the AMP-activated protein kinase (AMPK). AMPK is a highly conserved and ubiquitously expressed heterotrimeric enzyme complex (consisting of α, β and γ isoforms) that functions as a sensor of cellular energy status [25]. By inhibiting mitochondrial function leading to reductions in the cellular adenylate charge and subsequent activation of the kinase through the interactions with the AMPK gamma isoforms, metformin, an inexpensive and generally safe anti-diabetic drug, activates AMPK indirectly [25–27]. Of interest, intra-peritoneal injections of metformin were found to attenuate cystic kidney disease in *Pkd1* mutant mice by activating AMPK and inhibiting mTORC1 signalling [19]. These promising results have led to the testing of metformin for ADPKD in a phase II clinical trial [28]. However, reduced bioavailability (~50–60%) and gastrointestinal intolerance (in ~30% of patients) coupled with a high hepatic first-pass effect (i.e. liver concentrating a high percentage of drug after gut absorption) raise concerns that the maximal oral dose of metformin (i.e. 2·0 g/day) used clinically may not be sufficient for therapeutic AMPK activation in the kidney [29,30]. Thus, there is a need to develop more effective AMPK-based therapeutics which can be translated to treat patients with ADPKD.

In this study, we explored whether the addition of a second AMPK-activating drug to metformin would enhance its therapeutic effects for experimental treatment of ADPKD. One of these drugs was a recently approved type 2 diabetic medication, canagliflozin, also an indirect AMPK activator like metformin [31,32]. In addition, we also examined the effects of salsalate, a prodrug dimer of salicylate, which in contrast to metformin and canagliflozin, activates AMPK through direct interactions with the drug-binding domain of the AMPK β1 isoform [25,33]. Importantly, previous studies have indicated that given their distinct mechanisms for activating AMPK, there are synergies between metformin and salsalate therapy for treating fatty liver disease and suppressing mTOR in cancer cells [34,35]. All three drugs have excellent safety profile and may be appropriate for drug repurposing to treat ADKPD [36]. To examine the additive (metformin plus canagliflozin) or synergistic (metformin plus salsalate) effect of metformin combination therapy, we tested in this study the efficacy of oral treatment of (i) metformin, (ii) canagliflozin, (iii) salsalate, (iv) metformin plus canagliflozin, (v) metformin plus salsalate vs. (vi) untreated mutant control in an adult-onset *Pkd1* conditional deletion mouse model.

2. Materials and methods

2.1. Mouse experimental protocol

The experimental design of our study is shown in Fig. 1. All the study groups were run concurrently in one large experiment. We used the iKsp-*Pkd1*^{del} conditional knock-out (KO) mice on a C57BL6/J congenic background for the testing [10,37]. Twenty male mice/group were treated with tamoxifen (150 mg/kg, by oral gavage) at days P18 and P19 to inactivate *Pkd1* which will lead to renal failure at around 4 months of age. Drug treatment began on day P40. Metformin (AK-Scientific, # I506) was administered orally in drinking water at 1·5 mg/mL (or ~300 mg/kg/day); canagliflozin (MedChemExpress, # HY-10451) was administered orally at 10 mg/kg/day (62·5 mg/kg of food pellets (RM 3(E)), Special Diet Services); and salsalate (AK-Scientific, # F817) was administered orally at 400 mg/kg/day (2·5 g/kg of food pellets, Special Diet Services). As control, one group of mice received food pellets generated by the same protocol, but without any drug. Blood urea nitrogen (BUN) was measured weekly starting at day P75 using 30 μl blood samples from the tail vein (Reflotron technology, Roche). All mice with a BUN >20 mmol/L were considered to have ESRD and sacrificed; BUN of WT mice was ~9 mmol/L. When ~50% of the untreated mice reached ESRD at 111–115 days of age, all mice from the control and other treatment groups were sacrificed within 5 days. For mice with BUN >20 mmol/L, the time to ESRD was calculated by linear interpolation of the ages between the last two BUN measurements. The age at ESRD or at censoring (i.e. mice without ESRD at the time of their last BUN measurement between 111 and 115 days of age) was used for Kaplan Meier survival analysis. All animal experiments were approved by the Animal Experiment Committee of the Leiden University Medical Centre and the Commission Biotechnology in Animals of the Dutch Ministry of Agriculture, and performed in accordance to Directive 2010/63/ EU for animal experiments.

2.2. Measurement of drug and cAMP levels

We measured serum metformin levels by an in-house assay we developed using liquid chromatography tandem mass spectrometry (LC-MS/MS) at the Clinical Biochemistry Laboratory of the Toronto General Hospital (see Supplementary Information). We measured serum salicylate levels using a commercially available kit (Neogen Corporation) and

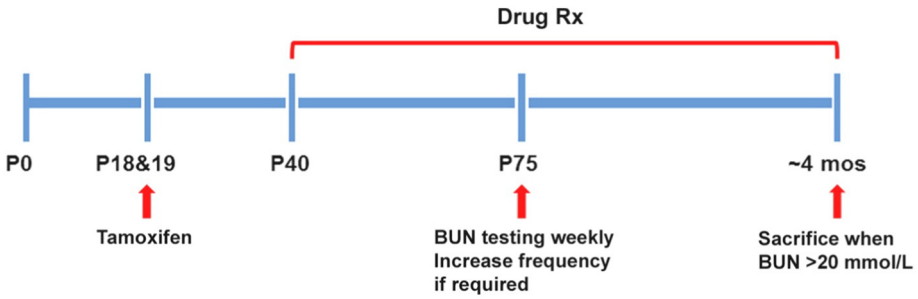

Fig. 1. Experimental protocol. Twenty male Tam-Ksp-*Pkd1*^{loxlox} mice/group were treated with tamoxifen at days P18 and P19 to inactivate *Pkd1* and drug treatment began on day P40 (Rx). Untreated mutant mice began to develop advanced kidney failure at around ~P105. BUN monitoring via tail-vein blood sampling began at P75 to identify those mice with kidney failure; all mice with a BUN >20 mmol/L were considered to have ESRD and sacrificed. When ~50% of the untreated mutant mice reached ESRD, all the mice from all study groups were sacrificed.

kidney tissue cAMP using the Direct cAMP ELISA kit (Enzo Life Sciences), according to the manufacturer instructions. Serum drug levels were measured in individual mutant mice after at least one month of treatment in the metformin group ($n = 20$) and salsalate group ($n = 21$) and at the time of sacrifice in the metformin group only ($n = 19$). Canagliflozin was not measured directly, but was expected to induce osmotic diuresis and hence, increased water intake was used as a surrogate marker of the drug effect. Indeed, we observed ~1·5 fold increased water intake in canagliflozin-treated mice.

2.3. Histological studies of kidney tissues

Kidneys were fixed in 4% buffered formaldehyde solution and embedded in paraffin. Periodic acid–Schiff (PAS) and Sirius Red staining was performed using standard protocols. F4/80 staining was used to detect macrophages. In brief, proteinase K antigen retrieval was used followed by a 20 min 0·12% H_2O_2 incubation step to block endogenous peroxidase. The sections were then incubated with rat anti-F4/80 (1:100; Serotec), followed by a second incubation step with anti-rat ImmPRESS™ (Vectorlabs). Immune reactions were revealed using diaminobenzidine as a chromogen and counterstained with hematoxylin, dehydrated, and mounted. Quantifications were done using Photoshop software as described previously [37]. Colour palettes were designed to select pixels specific for those within cysts, those of the red Sirius Red signal (large arteries were excluded from the analyses), or those of the brown F4/80 signal. The total number of pixels from the entire section (without cysts) and the total number of pixels from either the Sirius red or F4/80 signal were used to calculate the percentage of Sirius Red or F4/80 staining within the entire kidney section.

2.4. Gene expression and bioinformatics analysis

Using the Mouse Gene 2·0 ST Arrays (Affymetrix), we performed global gene expression profiling of 30 kidney samples (wild-type,

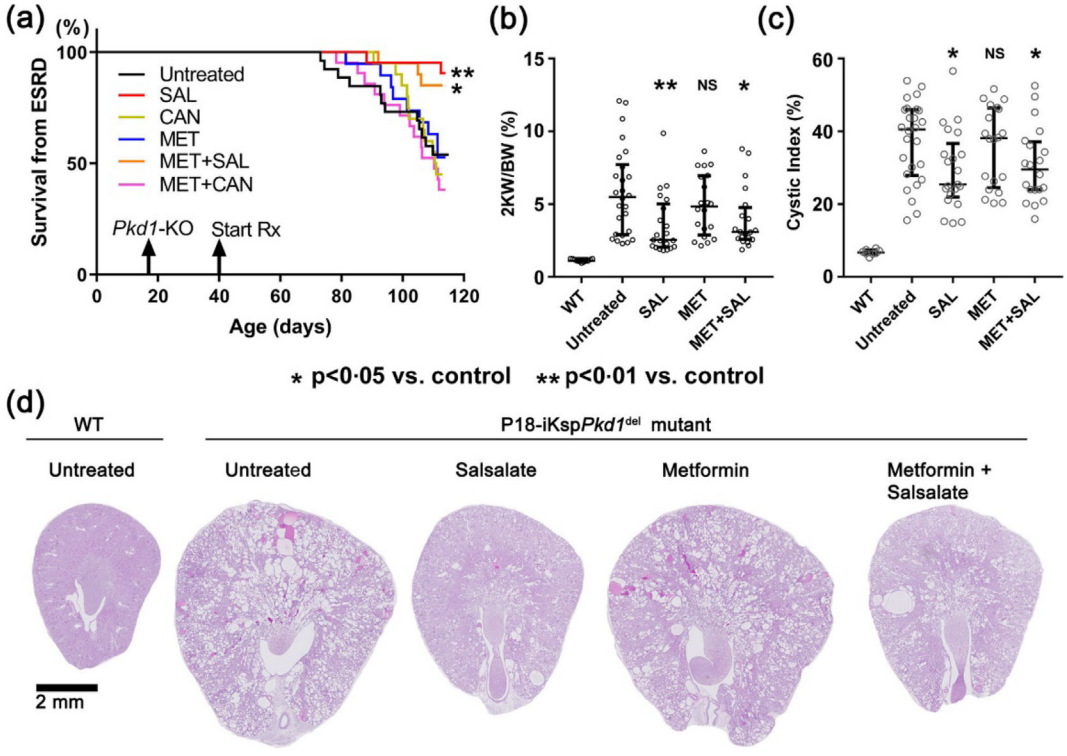

Fig. 2. Salsalate treatment slowed progression of polycystic kidney disease in iKsp-*Pkd1*^{del} mice. (a) Only treatment with salsalate (SAL) or metformin plus salsalate (MET+SAL) was associated with a significant improvement in kidney survival. Only treatment with salsalate or metformin plus salsalate was associated with a significant reduction in (b) the ratio of two-kidney weight to body weight (2KW/BW) and (c) cystic index. There was no difference between treatment with MET+SAL and SAL suggesting the therapeutic effect of the former treatment group was likely due to salsalate alone. (d) Representative histological kidney sections (i.e. the median) from different study groups. NS denotes not significant. Data presented as mean ± SEM; WT ($n = 8$), untreated ($n = 26$), SAL ($n = 21$), MET ($n = 19$), MET+SAL ($n = 20$).

$n = 7$; KO mice, $n = 12$, and KO mice treated by salsalate, $n = 11$) which were selected around the median of the cystic index from each group. Microarray gene expression studies were performed by the Centre for Applied Genomics Core at the Hospital for Sick Children (Toronto, Ontario, Canada). QC measures and filtering are detailed in the Supplementary Information and in Figs. S1, S4, and S5. Differentially expressed genes were split into two groups of up-regulated and down-regulated genes. The lists of up-regulated and down-regulated genes were each used for gene set enrichment analysis (GSEA). We used Enrichr as the primary tool for GSEA [38]. We used Benjamini-Hochberg (false discovery rate) FDR-adjusted *p*-values and *Z*-scores computed by Enrichr for the ranking of each gene set. Hierarchical clustering analysis and heatmap were performed using the DNA-Chip Analyzer (dChip) software package [39].

2.5. Western blot analysis

Protein extraction from whole kidney tissues for Western blot analysis are detailed in Supplementary Information. After collecting the supernatants from the kidney lysates, protein extracts were quantified using Protein Assay Kit (Bio-Rad) and then denatured in Laemmli sample buffer. Proteins were separated on TGX gradient gels (Bio-Rad) and then transferred onto PVDF membranes (Bio-Rad) by using Trans-Blot Turbo System (Bio-Rad). The membranes are incubated in blocking buffer (150 mM NaCl, 20 mM Tris, 5% skim milk, 0·1% Tween 20) for 60 min, and then incubated with primary antibodies at 4 °C overnight. Subsequently, primary antibody binding was detected with horseradish peroxidase (HRP)-conjugated anti-rabbit, or anti-mouse secondary antibodies, and proteins were visualized with an enhanced chemiluminescence detection kit (ECL; Bio-Rad or Cell Signalling Technology). For determination of phospho/total protein levels, immunoblots were first probed for phospho levels, then stripped at RT for 30 min using *Re*-Blot Plus Mild Antibody Stripping Solution (EMD Millipore) and re-probed overnight to detect total levels. Protein expression was quantified by densitometric analysis with ImageJ software (NIH, http://rsbweb.nih.gov/ij/) according to the guidelines. All the primary and secondary antibodies used for this study are listed in Supplementary Information.

2.6. Quantification of mitochondrial DNA copy number

Total DNA containing mitochondrial and nuclear DNA (nDNA) was isolated by using QIAamp DNA Mini Kit (Qiagen). We performed quantitative real-time PCR using Power SYBR® Green PCR Master Mix (Applied Biosystems) with primers specific to a mitochondria-encoded gene, 16S ribosomal RNA (16 s rRNA) (forward: 5′-CCGCAAGGGAAAGATGAAAGAC-3′; reverse: 5′-TCGTTTGGTTTCGGGGTTTC-3′) and a nuclear-encoded gene, B2m (forward: 5′- GCCGAACATACTGAACTGCTAC-3′; reverse: 5′- GTGAGCCAGGATATAGAAAGACC-3′), as previously described [40]. Mitochondrial DNA (mtDNA) copy number was estimated by the ratio of 16S rRNA/B2m.

2.7. Statistical analysis

Statistical analysis was performed using GraphPad Prism 7 software (San Diego, CA, USA). All results are expressed as dot-blots with median and interquartile ranges or mean ± SEM. Comparisons involving more than two groups were performed by one-way ANOVA followed by Tukey's or Dunnett's test post hoc; *p*-values corrected for multiple comparisons were reported. The Log Rank (Mantel-Cox) test was used for

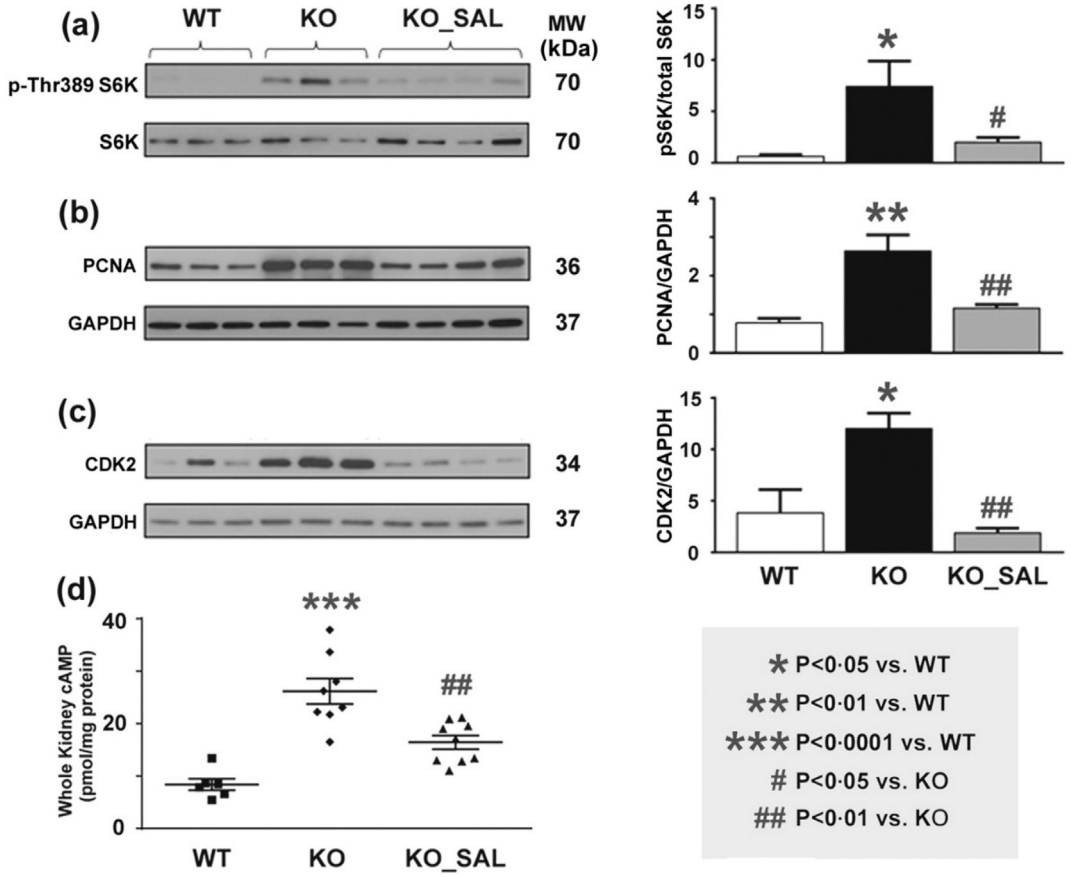

Fig. 3. Salsalate reversed multiple pathogenic mediators of cystic kidney disease in iKsp-*Pkd1*^{del} mice. Western blot analyses showed that kidneys from mutant *Pkd1* mice (compared to WT mice) displayed increased expression of protein markers for (a) mTORC1 activity (i.e. levels of pS6K), (b) cell proliferation (i.e. PCNA), (c) cell cycle progression (i.e. CDK2), and (d) cAMP; all these changes were significantly attenuated by salsalate treatment. Data presented as mean ± SEM. For kidney cAMP levels, WT (n = 7), KO ($n = 8$), SAL ($n = 9$).

the Kaplan Meier survival analyses. The fibrotic index and F4/80 index between salsalate-treated and untreated *Pkd1* mice were tested using unpaired Student's *t*-tests.

3. Results

3.1. Salsalate, but not metformin or canagliflozin, slowed polycystic kidney disease

The iKsp-*Pkd1*^{del} mice were treated with clinically relevant drug doses according to experimental protocol (Fig. 1; also see Materials and Methods). When 46% of untreated *Pkd1* mutant ('disease control') mice had reached ESRD by 111–115 days of age, all the mice from all study groups were sacrificed at that time. The mean serum metformin levels measured by LC-MS/MS in the mutant mice after at least one month of treatment ($n = 20$) and at the time of sacrifice ($n = 19$) were 14·6 (90%CI: 18·6–21·4) and 17.2 (90%CI: 14·1–20·3) μM, respectively. The median serum salicylate levels measured by ELISA in the mutant mice after at least one month of salsalate treatment ($n = 21$) was 222 (IQR: 108–372) μM. By comparison, the mean serum metformin and salicylate levels reported in diabetic patients on steady state clinical doses were 10 μmol/L and 1350 μmol/L, respectively.[29,30,41] Moreover, in a pilot study of 5 PKD patients on 1·5–2 g/day of oral metformin, we found a median serum metformin level of 9·8 [range: 1·34 to 18·8] μmol/L (see Supplementary Information). These data indicate that clinically relevant serum drug levels were achieved in the metformin- and salsalate-treated mutant mice. Here we show that treatment with salsalate or metformin plus salsalate was associated with a significant

Table 1
Top ranked dysregulated Reactome pathways enriched in *Pkd1* mutant mouse kidneys but attenuated by salsalate treatment.

Top 20 down-regulated Reactome pathways enriched in iKsp-*Pkd1*^{del} mouse kidneys but attenuated by salsalate treatment	Top down-regulated Reactome pathways enriched in iKsp-*Pkd1*^{del} (vs. WT) mice		Top up-regulated Reactome pathways in salsalate-treated (vs. untreated) iKsp-*Pkd1*^{del} mice	
	Adjusted P-value*	*Z*-score	Adjusted *P*-value*	Z-score
Metabolism	6·49E−82	−2·25	1·88E-69	−2·25
The citric acid (TCA) cycle and respiratory electron transport	6·94E−67	−1·97	7·30E-50	−1·97
Respiratory electron transport, ATP synthesis by chemiosmotic coupling, and heat production by uncoupling proteins	1·12E−51	−1·98	5·43E-38	−1·98
Respiratory electron transport	8·07E−46	−1·95	1·15E-37	−1·95
Complex I biogenesis	3·61E−31	−2·02	3·33E−23	−2·02
Metabolism of lipids and lipoproteins	1·12E−14	−2·13	6·39E-22	−2·19
Metabolism of amino acids and derivatives	5·32E−14	−2·15	2·12E-16	−2·22
Pyruvate metabolism and Citric Acid (TCA) cycle	1·21E−17	−1·78	1·29E-13	−1·81
Fatty acid, triacylglycerol, and ketone body metabolism	1·16E−09	−2·05	1·07E−12	−2·17
Branched-chain amino acid catabolism	1·24E−12	−1·84	1·30E−10	−2·03
Mitochondrial protein import	3·73E−16	−1·76	2·51E-09	−1·76
Mitochondrial Fatty Acid Beta-Oxidation	1·34E−09	−1·40	5·04E-09	−1·75
Citric acid cycle (TCA cycle)	9·13E−13	−1·84	3·08E-08	−1·92
Metabolism of water-soluble vitamins and cofactors	1·40E−15	−1·88	3·08E-08	−1·87
Peroxisomal lipid metabolism	3·75E−14	−1·99	3·68E-08	−1·99
Glyoxylate metabolism and glycine degradation	2·37E−11	−1·54	1·38E-07	−1·64
Histidine, lysine, phenylalanine, tyrosine, proline and tryptophan catabolism	5·41E−12	−1·66	3·56E-07	−1·70
Mitochondrial translation	3·82E−27	−2·07	4·45E-07	−1·96
Mitochondrial translation elongation	1·75E−26	−2·02	4·71E-07	−1·91
Mitochondrial translation initiation	1·92E−25	−1·98	4·71E-07	−1·88

Top 20 up-regulated Reactome pathways enriched in iKsp-*Pkd1*^{del} mouse kidneys but attenuated by salsalate treatment	Top up-regulated Reactome pathways enriched in iKsp-*Pkd1*^{del} (vs. WT) mice		Top down-regulated Reactome pathways in salsalate-treated (vs. untreated) iKsp-*Pkd1*^{del} mice	
	Adjusted P-value*	*Z*-score	Adjusted P-value*	Z-score
Immune system	1·01E−28	−2·23	3·12E−35	−2·23
Extracellular matrix organization	6·10E−24	−2·09	1·90E−33	−2·10
Hemostasis	1·44E−18	−2·10	1·51E−23	−2·13
Signalling by Rho GTPases	1·42E−25	−2·20	4·45E−22	−2·18
Cytokine signalling in immune system	2·67E−17	−2·34	1·91E−17	−2·37
Cell cycle, mitotic	2·92E−23	−2·44	3·04E−17	−2·43
RHO GTPase effectors	9·22E−19	−2·23	8·48E−17	−2·22
Axon guidance	9·37E−14	−2·28	8·95E−17	−2·30
Cell cycle	1·99E−25	−2·44	1·66E−16	−2·39
Developmental biology	2·90E−12	−2·27	1·77E−16	−2·30
Innate immune system	5·69E−15	−2·36	2·16E−16	−2·34
Integrin cell surface interactions	6·19E−11	−1·83	3·03E−15	−1·89
Platelet activation, signalling and aggregation	2·49E−12	−2·06	5·11E−15	−2·06
Cell-Cell communication	1·02E−09	−1·85	1·54E−13	−1·92
Non-integrin membrane-ECM interactions	8·67E−10	−1·81	5·97E−13	−1·89
Mitotic prometaphase	2·91E−14	−1·97	7·82E−12	−1·92
RHO GTPases activate formins	1·06E−12	−1·94	1·92E−11	−1·89
Interferon signalling	4·27E−11	−1·97	2·10E−11	−1·96
Platelet degranulation	3·35E−07	−1·58	7·99E−11	−1·77
Response to elevated platelet cytosolic Ca2+	2·03E−07	−1·61	9·23E−11	−1·75

* P-values computed by Fisher exact test and adjusted for multiple testing using the Benjamini-Hochberg method.

improvement in kidney survival (Fig. 2a) and reduction in cystic kidney disease severity (Fig. 2b-d). However, the therapeutic effects of salsalate vs. metformin plus salsalate did not differ, suggesting that the therapeutic effects in the latter group was due to salsalate alone. Of note, the therapeutic effect of salsalate was very strong, and comparable to that by oral tolvaptan treatment using the same model and protocol in a separate study (manuscript in preparation). By contrast, treatment with metformin, canagliflozin, alone or together was not effective (Figs. 2, S2). A concern of metformin treatment is its potential for gastrointestinal side-effects including anorexia and diarrhea which can cause volume depletion. However, our metformin-treated mice appeared well and gained weight similar to mice from the other experimental groups throughout the study (Fig. S3). Moreover, there was an excellent correlation between BUN and 2KW/BW (Fig. S4) suggesting the loss of GFR was related to the cystic disease burden. Since treatment with metformin or canagliflozin was not effective, we focused our mechanistic study on salsalate.

3.2. Salsalate attenuated pathogenic mediators in Pkd1 mutant mouse kidneys

Aberrant mTORC1 activation [16–22] and increased cAMP signalling [7,11,13] in cystic tissues are two well-validated pathogenic mechanisms driving cyst growth in ADPKD. In turn, both of these pathogenic mechanisms have been shown to increase cystic epithelial cell proliferation while increased cAMP signalling also drives cystic fluid secretion [11]. By Western blot analyses, we found that *Pkd1* mutant mouse kidneys (compared to wild type) displayed increased markers for

Table 2
Top ranked dysregulated biological processes enriched in *Pkd1* mutant mouse kidneys but attenuated by salsalate treatment.

Top 20 down-regulated biological processes enriched in iKsp-*Pkd1*^{del} mouse kidneys but attenuated by salsalate treatment	Top down-regulated biological processes enriched in iKsp-*Pkd1*^{del} (vs. WT) mice		Top up-regulated biological processes in salsalate-treated (vs. untreated) iKsp-*Pkd1*^{del} mice	
	Adjusted P-value*	*Z*-score	Adjusted *P*-value*	Z-score
Respiratory electron transport chain	6·90E−34	−1·36	4·96E−28	−1·36
Mitochondrial ATP synthesis coupled electron transport	3·35E−30	−1·90	4·74E−25	−1·90
Fatty acid beta-oxidation	2·82E−23	−1·52	1·12E−21	−1·53
Fatty acid catabolic process	4·99E−25	−1·82	2·29E−19	−1·83
Mitochondrial respiratory chain complex assembly	1·44E−29	−1·78	2·29E−19	−1·78
Mitochondrial respiratory chain complex I biogenesis	9·04E−27	−1·58	8·73E−19	−1·58
NADH dehydrogenase complex assembly	9·04E−27	−1·57	8·73E−19	−1·57
Mitochondrial respiratory chain complex I assembly	9·04E−27	−1·41	8·73E−19	−1·41
Mitochondrial electron transport, NADH to ubiquinone	2·54E−20	−2·72	2·41E−18	−2·72
Fatty acid oxidation	1·84E−19	−1·81	1·08E−14	−1·81
Monocarboxylic acid metabolic process	1·56E−11	−1·64	7·54E−11	−1·65
Dicarboxylic acid metabolic process	6·96E−12	−1·82	1·31E−10	−1·83
Cellular respiration	2·41E−15	−1·24	4·59E−10	−1·24
Cellular amino acid catabolic process	1·59E−11	−1·68	7·19E−10	−1·69
Branched-chain amino acid catabolic process	1·79E−11	−1·77	2·53E−09	−1·78
Branched-chain amino acid metabolic process	1·80E−09	−1·74	5·34E−09	−1·75
Fatty acid metabolic process	5·62E−10	−1·31	5·34E−09	−1·32
Fatty acid beta-oxidation using acyl-CoA dehydrogenase	4·92E−07	−2·31	1·06E−07	−2·32
Coenzyme metabolic process	8·55E−07	−2·44	1·39E−07	−2·48
Mitochondrial transport	4·26E−18	−1·33	5·67E−07	−1·33

Top 20 up-regulated biological processes enriched in iKsp-*Pkd1*^{del} mouse kidneys but attenuated by salsalate treatment	Top up-regulated biological processes enriched in iKsp-*Pkd1*^{del} (vs. WT) mice		Top down-regulated biological processes in salsalate-treated (vs. untreated) iKsp-*Pkd1*^{del} mice	
	Adjusted P-value*	Z-score	Adjusted P-value*	Z-score
Extracellular matrix organization	2·11E−27	−1·65	1·76E−35	−1·65
Cellular response to cytokine stimulus	5·98E−20	−1·17	6·33E−23	−1·17
Regulation of cell migration	1·98E−16	−1·27	8·07E−22	−1·27
Cytokine-mediated signalling pathway	1·05E−23	−1·34	1·42E−21	−1·34
Neutrophil mediated immunity	2·29E−08	−1·90	1·11E−15	−1·94
Neutrophil degranulation	4·15E−08	−1·96	1·53E−15	−2·01
Response to cytokine	1·22E−12	−1·28	1·53E−15	−1·28
Neutrophil activation involved in immune response	4·15E−08	−1·23	2·61E−15	−1·25
Regulation of apoptotic process	2·06E−11	−1·77	1·26E−14	−1·78
Positive regulation of gene expression	1·47E−13	−1·66	2·87E−13	−1·66
Transmembrane receptor protein tyrosine kinase signalling pathway	5·92E−14	−1·74	1·75E−12	−1·73
Toll-like receptor signalling pathway	2·55E−10	−1·29	1·75E−12	−1·29
Regulation of cell proliferation	6·56E−13	−1·13	2·57E−12	−1·12
Protein phosphorylation	1·50E−11	−1·09	1·77E−11	−1·09
Positive regulation of transcription, DNA-templated	8·62E−16	−1·71	2·36E−11	−1·69
Cellular response to mechanical stimulus	2·90E−10	−2·15	3·14E−11	−2·15
Positive regulation of cell migration	4·24E−08	−1·87	3·14E−11	−1·90
Pattern recognition receptor signalling pathway	1·17E−06	−1·45	3·14E−11	−1·47
Platelet degranulation	5·35E−06	−1·38	3·14E−11	−1·42
Positive regulation of cell proliferation	5·55E−09	−1·54	3·96E−11	−1·54

* P-values computed by Fisher exact test and adjusted for multiple testing using the Benjamini-Hochberg method.

mTORC1 activity (i.e. pS6K), cell proliferation (i.e. PCNA), and cell cycle progression (i.e. CDK2), as well as increased levels of cAMP; all of these changes were significantly attenuated by salsalate treatment (Fig. 3). However, we were unable to directly demonstrate increased AMPK activity which might be due to a number of technical issues (see Supplementary Information).

3.3. Salsalate treatment attenuated defective metabolism in Pkd1 mutant mouse kidneys

For a more comprehensive analysis of the molecular alterations, we performed gene expression profiling. Tables 1 and 2 highlight the key findings. Of interest, the top 20 down-regulated Reactome pathways and biological processes enriched in *Pkd1* mutant mouse kidneys but attenuated by salsalate treatment were all related to metabolism. These results confirm our previous data indicating a generalized defect in metabolism in *Pkd1* mutant kidneys with impaired fatty acid oxidation, amino acid catabolism and oxidative phosphorylation [42], all these changes were attenuated by salsalate (Fig. 4a). Reduced AMPK activity in cystic tissues is expected to decrease the activity of PGC-1α, a master regulator for the transcriptional factors PPARα, ERRα, and ERRγ; all play a critical role in fatty acid oxidation and mitochondrial biogenesis [43].By Western blot analysis, we confirmed reduced PGC-1α expression in *Pkd1* cystic kidneys, which was attenuated by salsalate (Fig. 4b). Our *in-silico* analysis also predicted *Ppara* and its heterodimeric partner, *Rxr*, as the top-ranked transcriptional factors inhibited in *Pkd1* mutant kidneys, but active in the salsalate treatment group (Table S1). Consistent with defective mitochondrial biogenesis in ADPKD [44–46], we found an inverse correlation between relative mitochondria copy number (using mtDNA/nDNA as a readout) and kidney weight/body weight in *Pkd1* cystic kidneys ($r = -0{\cdot}8$, $p < 0{\cdot}0001$) (Fig. 4c); the salsalate treated mice had higher mtDNA/nDNA ratios consistent with their milder PKD phenotype (Fig. 4d).

3.4. Salsalate treatment attenuated inflammation in Pkd1 mutant mouse kidneys

Recent studies have documented that kidney tissue inflammation can promote progression of experimental ADPKD. Specifically,

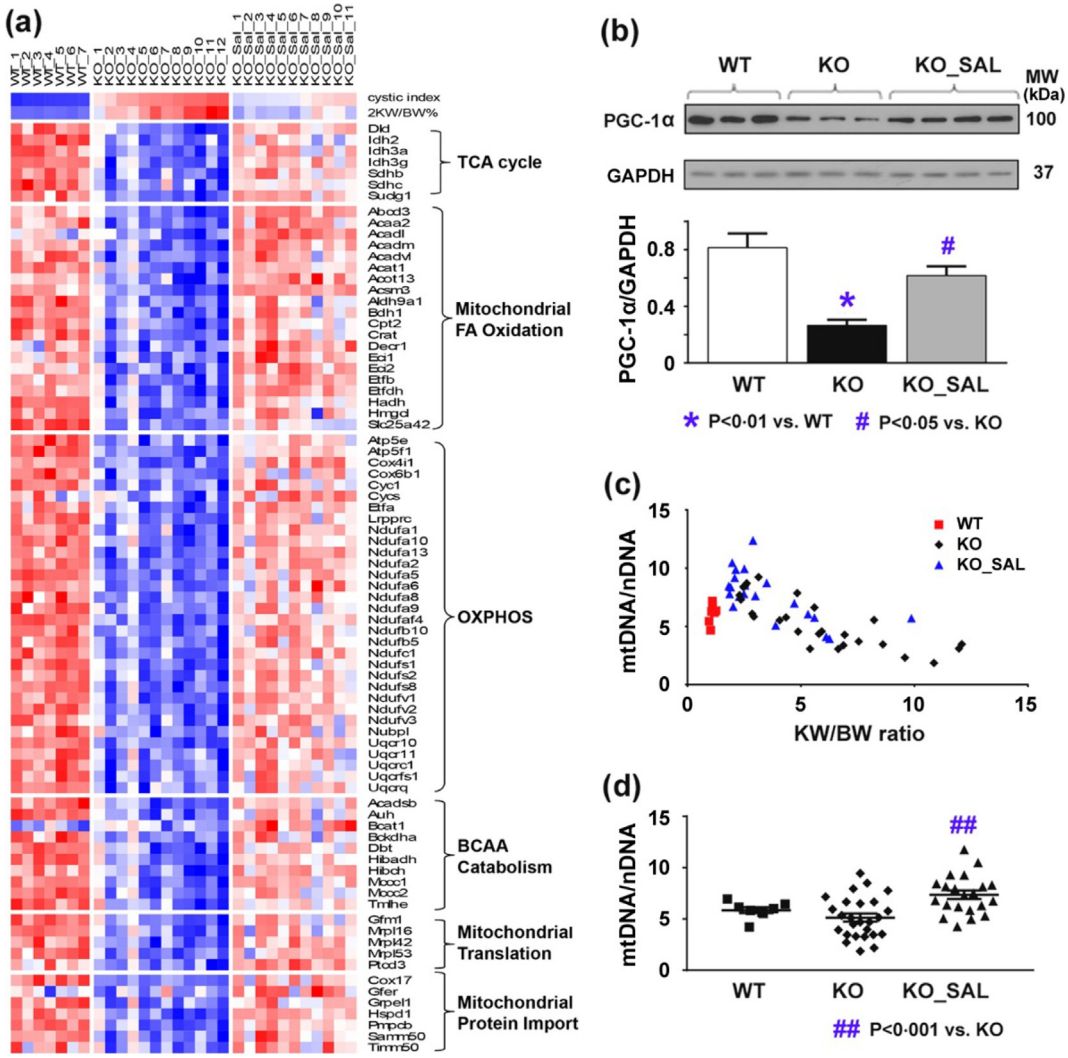

Fig. 4. Salsalate treatment improved defective metabolism in *Pkd1* mutant kidneys. (a) Gene expression profiling showing changes consistent with a generalized defective metabolism with reduced oxidative phosphorylation (OXPHOS) and mitochondrial biogenesis in mutant (compared to WT) *Pkd1* kidneys; these changes were attenuated by salsalate treatment (all changes shown were identified using a FDR adjusted *p*-value <0·01). Each column represents an individual kidney sample and each row represents the expression value of a specific gene; red indicates greater expression than the mean (white) value and blue, less than the mean value. (b) Western blot analysis confirming a decreased expression of PGC-1α in *Pkd1* mutant kidneys which was less pronounced by salsalate treatment. (c) An inverse correlation between mtDNA/nDNA and KW/BW in *Pkd1* mutant kidneys ($r = -0{\cdot}8$, $p < 0{\cdot}0001$) was noted consistent with defective mitochondrial biogenesis in ADPKD. (d) Salsalate treatment increased the ratio of mtDNA/nDNA in *Pkd1* mutant kidneys. Data presented as mean ± SEM. For kidney mtDNA qPCR, WT ($n = 8$), KO ($n = 26$), SAL ($n = 21$).

pharmacological and genetic manoeuvres depleting kidney tissue macrophage infiltration were shown to attenuate cystic disease severity [47,48]. Interestingly, multiple top upregulated Reactome pathways and biological processes enriched in *Pkd1* cystic kidneys but attenuated by salsalate were involved in immunity (Tables 1 and 2). By gene expression analysis, we found an increased expression of markers for damage-associated molecular patterns (DAMPs) and their receptors [49,50], macrophages, inflammation and fibrosis in *Pkd1* cystic kidneys; all of these changes were attenuated by salsalate treatment (Fig. 5a). NFκB is a key regulator of innate immunity [49] and its p65 (Rela) subunit was predicted to be a top-ranked activated transcriptional factor in *Pkd1* mutant kidneys, inhibited by salsalate (Table S1). We confirmed this finding by Western blot analysis (Fig. 5b). Consistent with our gene expression data, we found increased fibrosis and macrophage infiltration in *Pkd1* mutant kidneys, which were attenuated by salsalate treatment (Figs. 5c, d and 6).

4. Discussion

Given the concerns that therapeutic AMPK activation in the kidney might require a higher dose of oral metformin than can be achieved clinically [26,27,29,30], we tested metformin-based combination therapies for their additive (i.e. metformin plus canagliflozin) and synergistic (i.e. metformin plus salsalate) effects in an adult-onset *Pkd1*-deletion mouse model using dosages expected to yield clinically relevant drug levels [29–33]. We found that only salsalate (a prodrug dimer of salicylate) was effective in slowing PKD progression with serum salicylate levels at the lower clinical therapeutic range (i.e. 0·7–2·2 mmol/L) [41,51]. By contrast, metformin was not effective despite serum drug levels in the clinical therapeutic range (i.e. 10 μmol/L) [29,30]. Comparing our study to that by Takiar et al., which reported that *intra-peritoneal* metformin treatment was effective in slowing PKD [19], both studies used the same daily dose (i.e. 300 mg/kg). However, the bioavailability of oral metformin is only ~50% [26,27]. More recently, oral metformin treatment was reported to slow PKD progression in a miniature pig model using a dose of 41·7 mg/kg/day [52]. However, the estimated human equivalent dose used for this study is 2·77 g/day, which is higher than the usual dose (2 g/day) used clinically (see supplementary data) [53]. Differences in animal models and drug dosing in these studies may account for their discrepant results. However, serum metformin levels were not measured in these studies rendering them difficult to compare to our study. Preclinical studies that employ drug dosages modelling the clinical setting are more likely to have clinical relevance.

Increased mTORC1 [16–20] and cAMP signalling [11–13] in cystic tissues are two major pathogenic mechanisms driving cyst growth in ADPKD. In turn, activation of these signalling pathways have been shown to increase cystic epithelial cell proliferation in virtually all models of PKD[7] while increased cAMP signalling also drives cystic fluid secretion [11]. In this context, our results are consistent with upregulation of these signalling pathways in the *Pkd1* mutant mouse kidneys which was attenuated by salsalate treatment. Our findings suggest that salsalate may have an additive therapeutic effect with tolvaptan by targeting cAMP signalling [7,11–13].

Recent studies have shown that *Pkd1* cystic tissues display metabolic reprogramming consistent with a shift of the normal utilization of glucose through mitochondrial oxidative phosphorylation to aerobic glycolysis (a.k.a. the "Warburg effect") [20,21,54]. Instead of fully oxidizing one glucose molecule in the mitochondria to yield 36 ATP,

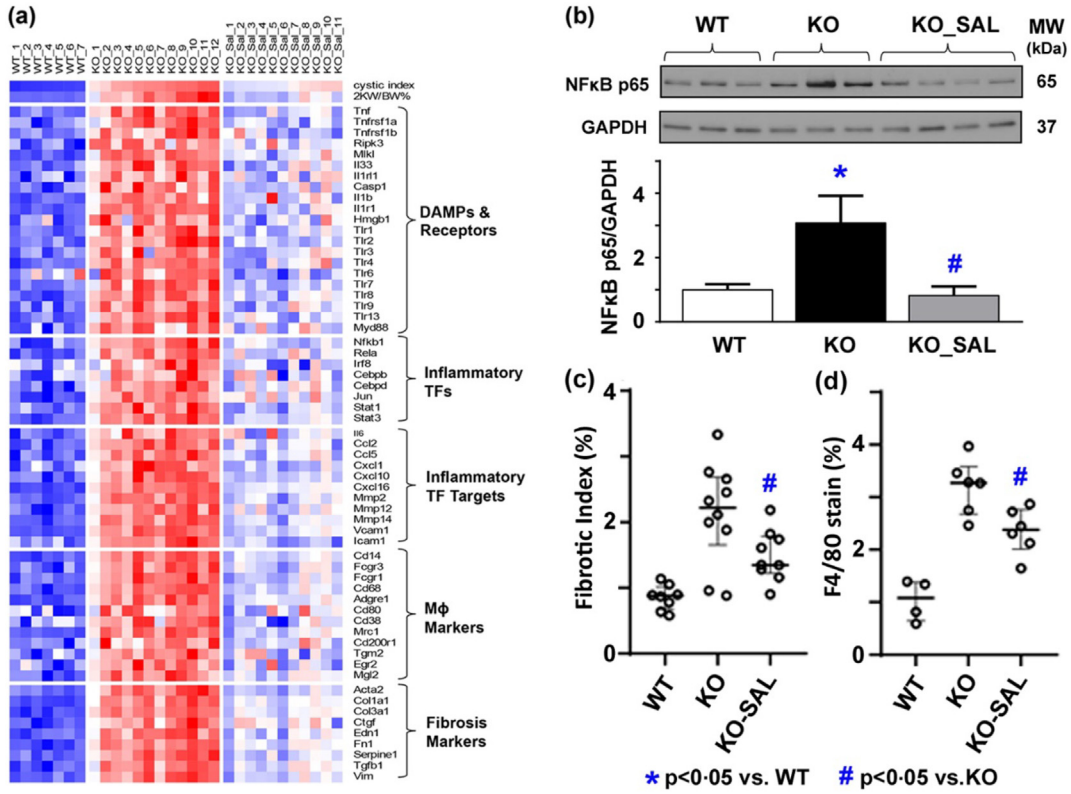

Fig. 5. Salsalate treatment reduced inflammation in *Pkd1* mutant kidneys. (a) Gene expression profiling showing an increased expression of markers for damage-associated molecular patterns (DAMPs) and their receptors, macrophages (MΦ), inflammation and fibrosis in *Pkd1* mutant kidneys. Each column represents an individual kidney sample and each row represents the expression value of a specific gene; red indicates greater expression than the mean (white) value and blue, less than the mean value. (b) Western blot analysis showing an increased expression of NFκB p65 in *Pkd1* mutant kidneys. Histological analysis showing increased (c) fibrosis by Sirius Red staining and (d) macrophage infiltration by F4/80 staining in *Pkd1* mutant kidneys; all these changes were less severe by salsalate treatment. TF denotes transcriptional factor. Data presented as mean ± SEM. For fibrotic index, WT ($n = 8$), KO ($n = 10$), SAL ($n = 21$); for F4/80 staining, WT ($n = 4$), KO ($n = 6$), SAL ($n = 6$).

cystic tissues prefer a metabolic pathway that generates only 4 ATP and 2 lactate molecules; the latter are then used to build macromolecules (nucleotides, proteins, lipids) to support cell proliferation [54]. In addition, defective fatty acid β-oxidation and altered mitochondrial function have been observed both in vitro and in animal models of ADPKD [44,55,56]. Indeed, the top 20 most down-regulated gene pathways in *Pkd1* mutant kidneys involved multiple metabolic processes ranging from tricarboxylic acid cycle, catabolism of fatty acids and amino acids, oxidative phosphorylation, to mitochondrial biogenesis; these changes suggest a generalized defective metabolism in *Pkd1* mutant kidneys which was attenuated by salsalate treatment. Consistent with the findings by Lakhia et al. [57], our data suggest that decreased activity of PPARα and PGC-1α (co-activator of PPARα) might contribute to the defective fatty acid oxidation and mitochondrial biogenesis in *Pkd1* cystic tissues. Of interest, fenofibrate, a PPARα agonist, was found in the former study to attenuate cystic kidney and liver disease in $Pkd1^{RC/RC}$ mice [57]. However, the clinical use of this drug is limited by its potential nephrotoxicity, especially for patients with chronic kidney disease [58].

Tissue injury can initiate an inflammatory response through the actions of damage-associated molecule patterns (DAMPs) which comprise a heterogeneous group of molecules released during cell necrosis, tissue repair and remodelling. In turn, DAMPs can trigger innate immunity by activating Toll-like receptors, purogenic receptors, or NLRP3 inflammasome [49]. Recent studies have shown that depletion of kidney macrophage infiltration by pharmacological and genetic manoeuvers attenuated *Pkd1* cystic disease severity [47,48]. We found that *Pkd1* cystic kidneys were enriched with increased expression of genes encoding for multiple necrosis-related DAMPs, alarmins and their receptors (e.g. Hmgb1 and Tlr — 2/4; Tnf and Tnfrsf1a; Il33 and Il1rl1; Il1b and Il1r1) as well as pathway proteins (e.g. multiple toll-like receptors (Tlrs), Myd88, Nfκb; Ripk3 and Mlkl) for innate immunity; all of these changes were attenuated by salsalate treatment [50]. Taken together, our data are consistent with an emerging body of literature suggesting necroinflammation can provide an auto-amplification loop of necrosis and inflammation that mediates progression of chronic kidney diseases [50]. Thus, salsalate treatment may confer a therapeutic effect for other kidney diseases beyond ADPKD.

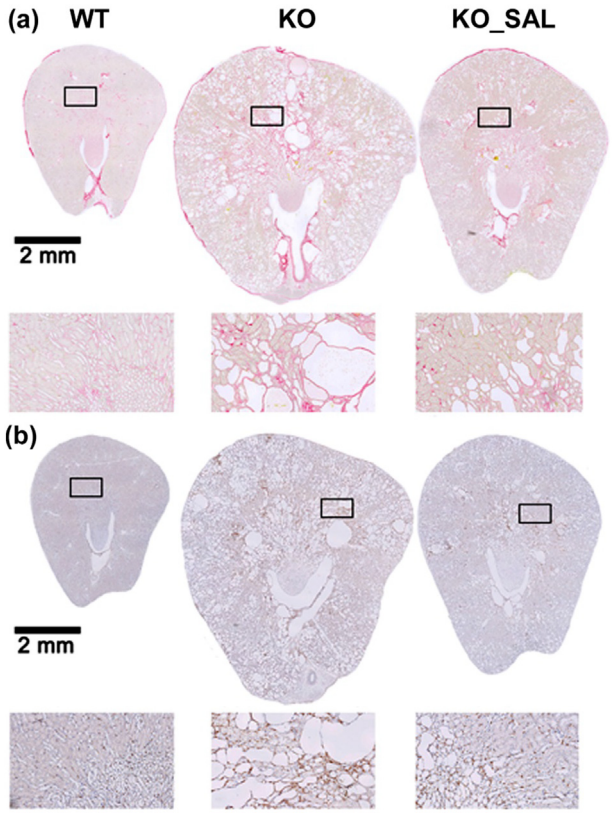

Fig. 6. Salsalate treatment reduced fibrosis and inflammation in *Pkd1* mutant kidneys. Representative kidney sections showing (a) Sirius Red staining for collagen deposition as early marker for fibrosis and (b) F4/80 staining for macrophage infiltration. Salsalate treated *Pkd1* mutant (KO_SAL) mice had less fibrosis and macrophage infiltration compared to untreated *Pkd1* mutant (KO) mice.

There are limitations or potential concerns in our study. First, our selection of samples closest to the median PKD severity for the gene expression studies might create bias by not including the outliers; nevertheless, this approach provides a valid assessment for the "average effect" of each study group. Second, metformin might result in volume depletion due to anorexia and diarrhea and a functional (i.e. renal vasoconstriction rather than structural damage) cause for increased BUN. However, our metformin-treated mice appeared well and gained weight similar to mice from other experimental groups throughout the study. There was also an excellent correlation between BUN and 2KW/BW which would not be expected if the rise of BUN was due to a functional cause. Nevertheless, there was a trend toward a steeper slope in the BUN vs. 2KW/BW correlation in the metformin-treated versus untreated mutant mice (Fig. S4), so a small functional effect on BUN could not be excluded. Lastly, since untreated mutant mice that reached ESRD were sacrificed earlier than the salsalate-treated mutant mice, there is a bias in our study design to underestimate the salsalate treatment effects when 2KW/BW and cystic index were used as the outcome readouts.

In conclusion, using dosages expected to yield clinically relevant serum drug levels we found that salsalate, but not metformin or canagliflozin, was highly effective in attenuating renal cystic disease in an adult-onset *Pkd1* mouse model. Of note, salsalate is a pro-drug which is released as two molecules of salicylate in the small intestine. Compared to aspirin (acetyl-salicylic acid), salicylate displays weak cyclooxygenase enzyme inhibitory activities at clinical dose and is associated with minimal bleeding risk and fewer GI side-effects [59,60]. Our observations of metabolic reprograming and inflammation in *Pkd1* cystic kidneys (as compared to wild-type control) which were attenuated by salsalate treatment are consistent with the putative mechanisms of action of salicylate to directly activate AMPK [33], uncouple oxidative phosphorylation [51], and strongly inhibit NF-κB [59]. The oral bioavailability of salsalate in humans is ~80%; most of the salicylate is metabolized by the liver and excreted by the kidneys. With an excellent safety profile, salsalate, at concentrations capable of activating AMPK, has been used for over five decades for the treatment of arthritis and more recently re-purposed for testing in phase 2 clinical trials of type 2 diabetes and cardiovascular disease [59,60]. These features, together with the results of our study, suggest that salsalate is a highly promising candidate for drug repurposing and clinical testing in ADPKD.

Author contributions

W.N.L., X.W.S., I.A.I., G.S., D.J.M.P., and Y.P. designed the study; W.N.L., X.W.S. and A.A.K. performed the study, analyzed the data, produced the figures and drafted the paper; A.B. developed the assays for and measured serum metformin levels; all the authors have read, edited and approved the final version of the manuscript.

Declaration of Competing Interest

Y.P. has served as consultant and received honoraria from Otsuka and Vertex Pharmaceutical. D.P. has served as consultant and received honorarium from Mironid. All other authors have nothing to disclose.

Acknowledgments

This work was supported in part by grants from the Canadian Institutes of Health Research (CIHR) Strategy for Patient Oriented Research

(SPOR) program in Chronic Kidney Disease (CAN-SOLVE CKD SCA-145103), Polycystic Kidney Disease Foundation of Canada (to Y.P. and D.J.M.P.), and Dutch Kidney Foundation (NSN 15OKG01 to W.N.L. and 17PhD02 to D.J.M.P. and W.N.L.). Some of the equipment used in this study was supported by the 3D (Diet, Digestive Tract and Disease) Centre funded by the Canadian Foundation for Innovation and Ontario Research Fund, project number 19442 and 30961.

Appendix A. Supplementary data

Supplementary data to this article can be found online at https://doi.org/10.1016/j.ebiom.2019.08.041.

References

[1] Lanktree MB, Haghighi A, Guiard E, et al. Prevalence estimates of polycystic kidney and liver disease by population sequencing. J Am Soc Nephrol 2018;29(10):2593–600.
[2] Peters DJ, Sandkuijl LA. Genetic heterogeneity of polycystic kidney disease in Europe. Contrib Nephrol 1992;97:128–39.
[3] Hwang YH, Conklin J, Chan W, et al. Refining genotype-phenotype correlation in autosomal dominant polycystic kidney disease. J Am Soc Nephrol 2016;27(6):1861–8.
[4] Cornec-Le Gall E, Audrézet MP, Chen JM, et al. Type of PKD1 mutation influences renal outcome in ADPKD. J Am Soc Nephrol 2013;24(6):1006–13.
[5] Heyer CM, Sundsbak JL, Abebe KZ, et al. Predicted mutation strength of nontruncating PKD1 mutations aids genotype-phenotype correlations in autosomal dominant polycystic kidney disease. J Am Soc Nephrol 2016;27(9):2872–84.
[6] Grantham JJ, Mulamalla S, Swenson-Fields KI. Why kidneys fail in autosomal dominant polycystic kidney disease. Nat Rev Nephrol 2011;7(10):556–66.
[7] Harris PC, Torres VE. Genetic mechanisms and signaling pathways in autosomal dominant polycystic kidney disease. J Clin Invest 2014;124(6):2315–24.
[8] Ong AC, Harris PC. A polycystin-centric view of cyst formation and disease: the polycystins revisited. Kidney Int 2015;88(4):699–710.
[9] Fedeles SV, Gallagher AR, Somlo S. Polycystin−1: a master regulator of intersecting cystic pathways. Trends Mol Med 2014;20(5):251–60.
[10] Leonhard WN, Happe H, Peters DJ. Variable cyst development in autosomal dominant polycystic kidney disease: the biologic context. J Am Soc Nephrol 2016;27(12):3530–8.
[11] Grantham JJ. Lillian Jean Kaplan international prize for advancement in the understanding of polycystic kidney disease. Understanding polycystic kidney disease: a systems biology approach *Kidney Int* 2003;64(4):1157–62.
[12] Gattone VH, Wang X, Harris PC, Torres VE. Inhibition of renal cystic disease development and progression by a vasopressin V2 receptor antagonist. Nat Med 2003;9(10):1323–6.
[13] Torres VE, Wang X, Qian Q, Somlo S, Harris PC, Gattone VH. Effective treatment of an orthologous model of autosomal dominant polycystic kidney disease. Nat Med 2004;10(4):363–4.
[14] Torres VE, Chapman AB, Devuyst O, et al. Tolvaptan in patients with autosomal dominant polycystic kidney disease. N Engl J Med 2012;367(25):2407–18.
[15] Torres VE, Chapman AB, Devuyst O, et al. Tolvaptan in later-stage autosomal dominant polycystic kidney disease. N Engl J Med 2017;377(20):1930–42.
[16] Shillingford JM, Murcia NS, Larson CH, et al. The mTOR pathway is regulated by polycystin−1, and its inhibition reverses renal cystogenesis in polycystic kidney disease. Proc Natl Acad Sci U S A 2006;103(14):5466–71.
[17] Shillingford JM, Piontek KB, Germino GG, Weimbs T. Rapamycin ameliorates PKD resulting from conditional inactivation of Pkd1. J Am Soc Nephrol 2010;21(3):489–97.
[18] Novalic Z, van der Wal AM, Leonhard WN, et al. Dose-dependent effects of sirolimus on mTOR signaling and polycystic kidney disease. J Am Soc Nephrol 2012;23(5):842–53.
[19] Takiar V, Nishio S, Seo-Mayer P, et al. Activating AMP-activated protein kinase (AMPK) slows renal cystogenesis. Proc Natl Acad Sci U S A 2011;108(6):2462–7.
[20] Rowe I, Chiaravalli M, Mannella V, et al. Defective glucose metabolism in polycystic kidney disease identifies a new therapeutic strategy. Nat Med 2013;19(4):488–93.
[21] Chiaravalli M, Rowe I, Mannella V, et al. 2-deoxy-d-glucose ameliorates PKD progression. J Am Soc Nephrol 2016;27(7):1958–69.
[22] Warner G, Hein KZ, Nin V, et al. Food restriction ameliorates the development of polycystic kidney disease. J Am Soc Nephrol 2016;27(5):1437–47.
[23] Serra AL, Poster D, Kistler AD, et al. Sirolimus and kidney growth in autosomal dominant polycystic kidney disease. N Engl J Med 2010;363(9):820–9.
[24] Walz G, Budde K, Mannaa M, et al. Everolimus in patients with autosomal dominant polycystic kidney disease. N Engl J Med 2010;363(9):830–40.
[25] Steinberg GR, Carling D. AMP-activated protein kinase: the current landscape for drug development. Nat Rev Drug Discov 2019;18:527–51.
[26] Pernicova I, Korbonits M. Metformin–mode of action and clinical implications for diabetes and cancer. Nat Rev Endocrinol 2014;10(3):143–56.
[27] Foretz M, Guigas B, Bertrand L, Pollak M, Viollet B. Metformin: from mechanisms of action to therapies. Cell Metab 2014;20(6):953–66.
[28] Seliger SL, Abebe KZ, Hallows KR, et al. A randomized clinical trial of metformin to treat autosomal dominant polycystic kidney disease. Am J Nephrol 2018;47(5):352–60.
[29] He L, Wondisford FE. Metformin action: concentrations matter. Cell Metab 2015;21(2):159–62.
[30] Chandel NS, Avizonis D, Reczek CR, et al. Are metformin doses used in murine cancer models clinically relevant? Cell Metab 2016;23(4):569–70.
[31] Hawley SA, Ford RJ, Smith BK, et al. The Na+/glucose cotransporter inhibitor canagliflozin activates AMPK by inhibiting mitochondrial function and increasing cellular AMP levels. Diabetes 2016;65(9):2784–94.
[32] Villani LA, Smith BK, Marcinko K, et al. The diabetes medication Canagliflozin reduces cancer cell proliferation by inhibiting mitochondrial complex-I supported respiration. Mol Metab 2016;5(10):1048–56.
[33] Hawley SA, Fullerton MD, Ross FA, et al. The ancient drug salicylate directly activates AMP-activated protein kinase. Science 2012;336(6083):918–22.
[34] Ford RJ, Fullerton MD, Pinkosky SL, et al. Metformin and salicylate synergistically activate liver AMPK, inhibit lipogenesis and improve insulin sensitivity. Biochem J 2015;468(1):125–32.
[35] O'Brien AJ, Villani LA, Broadfield LA, et al. Salicylate activates AMPK and synergizes with metformin to reduce the survival of prostate and lung cancer cells ex vivo through inhibition of de novo lipogenesis. Biochem J 2015;469(2):177–87.
[36] Padovano V, Podrini C, Boletta A, Caplan MJ. Metabolism and mitochondria in polycystic kidney disease research and therapy. Nat Rev Nephrol 2018;14(11):678–87.
[37] Leonhard WN, Kunnen SJ, Plugge AJ, et al. Inhibition of activin signaling slows progression of polycystic kidney disease. J Am Soc Nephrol 2016;27(12):3589–99.
[38] Kuleshov MV, Jones MR, Rouillard AD, et al. Enrichr: a comprehensive gene set enrichment analysis web server 2016 update. Nucleic Acids Res 2016;44(W1):W90–7.
[39] Li C, Hung Wong W. Model-based analysis of oligonucleotide arrays: model validation, design issues and standard error application. Genome Biol 2001;2(8)(RESEARCH0032).
[40] Quiros PM, Goyal A, Jha P, Auwerx J. Analysis of mtDNA/nDNA ratio in mice. Curr Protoc Mouse Biol 2017;7(1):47–54.
[41] Fleischman A, Shoelson SE, Bernier R, Goldfine AB. Salsalate improves glycemia and inflammatory parameters in obese young adults. Diabetes Care 2008;31(2):289–94.
[42] Malas TB, Formica C, Leonhard WN, et al. Meta-analysis of polycystic kidney disease expression profiles defines strong involvement of injury repair processes. Am J Physiol Renal Physiol 2017;312(4):F806–17.
[43] Fan W, Evans R. PPARs and ERRs: molecular mediators of mitochondrial metabolism. Curr Opin Cell Biol 2015;33:49–54.
[44] Padovano V, Kuo IY, Stavola LK, et al. The polycystins are modulated by cellular oxygen-sensing pathways and regulate mitochondrial function. Mol Biol Cell 2017;28(2):261–9.
[45] Ishimoto Y, Inagi R, Yoshihara D, et al. Mitochondrial abnormality facilitates cyst formation in autosomal dominant polycystic kidney disease. Mol Cell Biol 2017;37:e00337–417.
[46] Hajarnis S, Lakhia R, Yheskel M, et al. microRNA−17 family promotes polycystic kidney disease progression through modulation of mitochondrial metabolism. Nat Commun 2017;8:14395.
[47] Karihaloo A, Koraishy F, Huen SC, et al. Macrophages promote cyst growth in polycystic kidney disease. J Am Soc Nephrol 2011;22(10):1809–14.
[48] Chen L, Zhou X, Fan LX, et al. Macrophage migration inhibitory factor promotes cyst growth in polycystic kidney disease. J Clin Invest 2015;125(6):2399–412.
[49] Anders HJ, Schaefer L. Beyond tissue injury-damage-associated molecular patterns, toll-like receptors, and inflammasomes also drive regeneration and fibrosis. J Am Soc Nephrol 2014;25(7):1387–400.
[50] Mulay SR, Linkermann A, Anders HJ. Necroinflammation in kidney disease. J Am Soc Nephrol 2016;27(1):27–39.
[51] Smith BK, Ford RJ, Desjardins EM, et al. Salsalate (salicylate) uncouples mitochondria, improves glucose homeostasis, and reduces liver lipids independent of AMPK-β1. Diabetes 2016;65(11):3352–61.
[52] Lian X, Wu X, Li Z, et al. The combination of metformin and 2-deoxyglucose significantly inhibits cyst formation in miniature pigs with polycystic kidney disease. Br J Pharmacol 2019;176(5):711–24.
[53] U.S. Department of Health and Human Services, Food and Drug Administration. Center for drug evaluation and research. Guidance for industry: Estimating the maximum safe starting dose in initial clinical trials for therapeutics in adult healthy volunteers; July 2005.
[54] Vander Heiden MG, Cantley LC, Thompson CB. Understanding the Warburg effect: the metabolic requirements of cell proliferation. Science 2009;324(5930):1029–33.
[55] Menezes LF, Lin CC, Zhou F, Germino GG. Fatty acid oxidation is impaired in an orthologous mouse model of autosomal dominant polycystic kidney disease. EBioMedicine 2016;5:183–92.
[56] Lin CC, Kurashige M, Liu Y, et al. A cleavage product of Polycystin-1 is a mitochondrial matrix protein that affects mitochondria morphology and function when heterologously expressed. Sci Rep 2018;8(1):2743.
[57] Lakhia R, Yheskel M, Flaten A, Quittner-Strom EB, Holland WL, Patel V. PPARalpha agonist fenofibrate enhances fatty acid beta-oxidation and attenuates polycystic kidney and liver disease in mice. Am J Physiol Renal Physiol 2018;314(1):F122–31.
[58] Attridge RL, Frei CR, Ryan L, Koeller J, Linn WD. Fenofibrate-associated nephrotoxicity: a review of current evidence. Am J Health Syst Pharm 2013;70(14):1219–25.
[59] Anderson K, Wherle L, Park M, Nelson K, Nguyen L. Salsalate, an old, inexpensive drug with potential new indications: a review of the evidence from 3 recent studies. Am Health Drug Benefits 2014;7(4):231–5.
[60] Steinberg GR, Dandapani M, Hardie DG. AMPK: mediating the metabolic effects of salicylate-based drugs? Trends Endocrinol Metab 2013;24(10):481–7.